Available online at www.sciencedirect.com
ScienceDirect
Journal of Computational Physics 226 (2007) 354–378
JOURNAL OF COMPUTATIONAL PHYSICS
www.elsevier.com/locate/jcp

On the Huygens absorbing boundary conditions for electromagnetics

Jean-Pierre Bérenger *

Centre d'Analyse de Défense, 16 bis, Avenue Prieur de la Côte d'Or, 94110 Arcueil, France

Received 16 January 2007; received in revised form 12 April 2007; accepted 13 April 2007
Available online 21 April 2007

Abstract

A new absorbing boundary condition (ABC) is presented for the solution of Maxwell equations in unbounded spaces. Called the Huygens ABC, this condition is a generalization of two previously published ABCs, namely the multiple absorbing surfaces (MAS) and the re-radiating boundary condition (rRBC). The properties of the Huygens ABC are derived theoretically in continuous spaces and in the finite-difference (FDTD) discretized space. A solution is proposed to render the Huygens ABC effective for the absorption of evanescent waves. Numerical experiments with the FDTD method show that the effectiveness of the Huygens ABC is close to that of the PML ABC in some realistic problems of numerical electromagnetics. It is also shown in the paper that a combination of the Huygens ABC with the PML ABC is very well suited to the solution of some particular problems.

MSC: 35Q60; 35R35; 65N22; 78A40; 78M10; 78M20

Keywords: Absorbing boundary condition; Operator; Huygens; FDTD; Electromagnetics; Free space; Numerical method

1. Introduction

In recent years, two novel absorbing boundary conditions (ABC) appeared in the literature, for use in numerical electromagnetics with the finite-difference time-domain (FDTD) method. These ABCs are the multiple absorbing surfaces (MAS) condition [1], and the re-radiating boundary condition (rRBC) [2,3]. They were developed independently and formulated in slightly different manners, but both rely on the same basic principle that consists of cancelling the outgoing field leaving the domain by means of equivalent currents that radiate a field equal in magnitude and opposite in sign to the field to be cancelled.

The principle of the MAS and rRBC is then simple and attractive. Unfortunately, some difficulties arise as implementing them, because the outgoing field on the surface where the equivalent currents are impressed,

* Fax: +33 1 42 31 90 24.
E-mail address: berenger@cad.etca.fr

0021-9991/$ - see front matter
doi:10.1016/j.jcp.2007.04.008

called the Huygens surface [4], cannot be known rigorously. An operator is used to obtain an estimate of the equivalent currents. From this, the cancellation is not perfect, resulting in a certain amount of reflection from the proposed ABCs.

In this paper, we revisit this kind of ABCs. We consider more general ABCs, called Huygens ABCs (HABCs), that hold as special cases the MAS and the rRBC. We derive theoretical properties of the Huygens ABCs in continuous spaces as well as in the discrete FDTD space. This permits results and observations in [1–3] to be interpreted. Especially, we show that the residual field radiated outside the Huygens surface is the time derivative of the outgoing field, while the field reflected towards the inner domain is integrated on time as it passes back through the Huygens surface. We also show that the overall reflection from a HABC is equal, rigorously, to the reflection from the ABC formed with the operator used to estimate the equivalent currents. This is true for both traveling and evanescent waves. From this, methods [1–3], and more generally any HABC, cannot be viewed as novel ABCs. They are only alternative implementations of ABCs based on use of operators, for example alternative implementations of Higdon operator ABCs [5,6]. In consequence, ABCs [1–3] suffer from the same drawbacks as the operator ABCs. The most important is the strong reflection of the evanescent waves present in many problems of electromagnetics solved with numerical methods. This is verified in this paper with a FDTD experiment.

In the last part of the paper we show that Huygens ABCs are of valuable interest in some problems of numerical electromagnetics, despite of their equivalence to previously known operator ABCs. As shown in [1–3], high-order HABCs can be easily implemented by juxtaposing several one-order HABCs, without the stability problems faced when implementing high-order operator ABCs. However, the operators used in [1–3] are only designed to absorb traveling waves, they reflect in totality evanescent waves, so that the domain of application of the MAS [1] and rRBC [2,3] is probably narrow. We suggest two alternative ways to apply Huygens ABCs in an effective manner in realistic applications of numerical electromagnetics. The first way relies on the introduction of operators designed to absorb evanescent waves. By means of HABCs they can be easily combined with such traditional operators as Higdon operators. This permits effective absorption of both traveling and evanescent waves present in many problems, like using the complex frequency shifted (CFS) PML ABC [7,8]. This is illustrated with a waveguide problem using the FDTD method. The second suggested use of HABCs relies on their easy combination with the PML ABC. This is of interest in certain problems where both traveling waves and evanescent waves are present at low frequency. Then, a HABC placed in front of a CFS PML permits the traveling waves to be absorbed at low frequency, where the CFS PML is transparent to these waves [7,8]. This is discussed in detail and illustrated in the paper with a FDTD experiment.

2. Principle of the absorbing boundary condition based on use of a Huygens surface

In electromagnetics, the equivalence theorem states that the field produced within a given part of space by sources located outside this part can be reproduced by impressing the following electric and magnetic current densities upon the surface separating the two parts:

$$\vec{\boldsymbol{J}}_s = \vec{\boldsymbol{n}} \times \vec{\boldsymbol{H}}_i \tag{1a}$$

$$\vec{\boldsymbol{K}}_s = -\vec{\boldsymbol{n}} \times \vec{\boldsymbol{E}}_i \tag{1b}$$

where $\boldsymbol{n}$ is the unit vector normal to the surface, oriented in the direction opposite to the sources, and $\boldsymbol{E}_i$ and $\boldsymbol{H}_i$ are the fields that would exist upon the surface if the sources were present. The surface where equivalent currents are set is called a Huygens surface [4]. The equivalent currents radiate no field in the part of space where the sources are present. This permits incident waves to be enforced in finite methods [4] and is a requirement for achieving reflectionless Huygens ABCs.

An important remark can be done about the equivalent currents (1). If the orientation of the unit vector were reversed, that is the unit vector oriented towards the sources, the sign of the equivalent currents would be also reversed, so that the radiated field would be opposite to the field radiated by the sources. In a different context [9], such a Huygens surface whose unit vector in (1) is opposite to its physical orientation has been called an anti-Huygens surface. In the context of the Huygens ABC, a fundamental consequence of this

remark is that the Huygens surface designed to radiate fields whose sources are inside the enclosed domain will act as an anti-Huygens surface for the field reflected back towards this domain.

Consider now a part of space where the Maxwell equations are solved with such finite methods as the FDTD method or the finite element method (FEM). To simulate the free space surrounding the computational domain, an ABC is needed so as to absorb the outgoing field. The idea used in [1–3] consists of surrounding the domain of interest with a Huygens surface (Fig. 1) that radiates a field equal in magnitude and opposite in sign to the physical outgoing field. This can be realized by impressing electric and magnetic current densities $\boldsymbol{J}_s$ and $\boldsymbol{K}_s$ from (1), with $\boldsymbol{H}_i$ and $\boldsymbol{E}_i$ equal to the opposite of the outgoing field. In theory, the sum of the physical field with the impressed field equals zero, so that the actual field outside the Huygens surface is zero. No additional ABC is needed on the outer boundary of the domain because no field reaches this boundary. Moreover, currents $\boldsymbol{J}_s$ and $\boldsymbol{K}_s$ radiate no field inside the Huygens surface, so that there is no reflected field in the region of interest. In theory, the ABC is perfect.

In the actual implementation of this simple idea, things are a little different, because the field $(\boldsymbol{E}_i, \boldsymbol{H}_i)$ that would be present in the absence of the Huygens surface cannot be computed at the exact location of the Huygens surface. This can be viewed easily with the FDTD method. More fundamentally, in continuous spaces this is because the field is discontinuous through the Huygens surface. Another way to be convinced that the outgoing field on the Huygens surface cannot be known a priori is as follows: If this field were known exactly, we could impress it as a boundary condition. This would be a perfect ABC.

Thus, in order to implement the opposite field using (1), an estimate of the outgoing field at the Huygens surface location must be computed. Both in [1–3], this field is obtained from values of the field at inner FDTD nodes close to the Huygens surface. In [1] a Higdon operator is used. Such operators [5,6] have been designed to be used as an ABC. In [2,3] the field is evaluated more simply as the value at the closest inner node at the previous time step. Using such estimates the cancellation of the outgoing field is not perfect. A residual small field is radiated outside the Huygens surface. If the domain is ended with a perfect electric condition (PEC) the small field is reflected back towards the Huygens surface. Unfortunately, this small field is then amplified as it passes through the Huygens surface. It was shown in [1] in the case of the first-order Higdon operator that the overall reflected field is equal to the field that would be reflected if this operator were implemented as an operator ABC on the boundary of the domain. In this paper, we show both in the continuous space and in the discretized FDTD space that this is also true with any operator used to estimate the outgoing field at the Huygens surface location. From this, the most important conclusion of the present paper is that any Huygens ABC

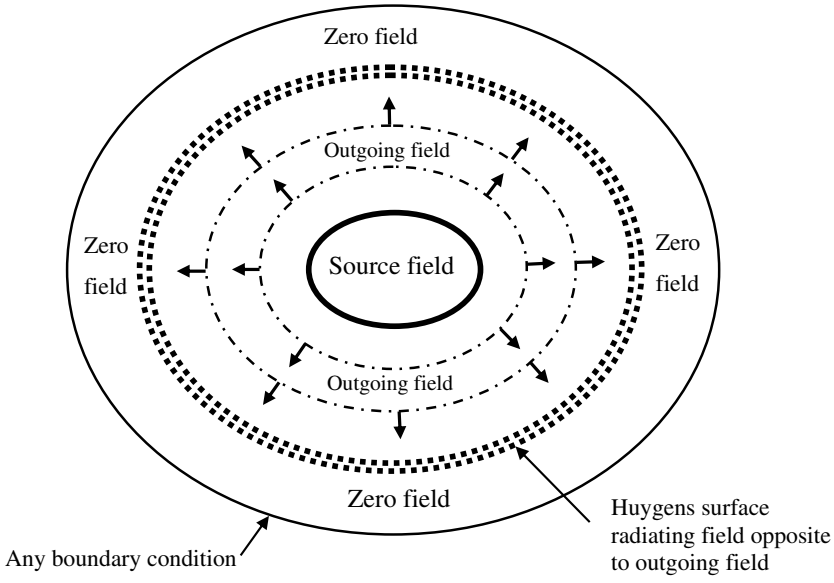

Fig. 1. The principle of the Huygens absorbing boundary condition.

is equivalent, in theory, to an operator ABC. However, this does not mean that Huygens ABCs are of no interest for numerical electromagnetics, as it will be shown in the last part of the paper.

3. The Huygens absorbing boundary condition in the continuous space

3.1. The Huygens ABC with the elementary operator

Let us consider the one-dimensional case depicted in Fig. 2a. An incident wave $U_{i+}(t - x/c)$ travels in x direction, where U is either E or H fields and c is the speed of light. In order to cancel the incident field, we wish that a Huygens surface generates at location x_c a field equal in magnitude and opposite in sign to the incident field. Unfortunately, this cannot be achieved rigorously, because the total field is discontinuous at x_c so that the exact incident field is not known at this location. We can only estimate $U_{i+}(x_c, t)$ in function of $U_{i+}(x, t)$ to the left of x_c. To this end, we assume that the field impressed in the equivalent currents (1) is a linear function of the actual field U_a present at several times and several locations to the left of x_c. Denoting this field as $\widetilde{U}(x_c, t)$, this can be written as

$$\widetilde{U}(x_c, t) = \sum_{k=1}^{N} a_k U_a(x_c - \delta x_k, t - \delta t_k) \tag{2}$$

where $\delta x_k > 0$, $\delta t_k \geqslant 0$, and

$$\sum_{k=1}^{N} a_k = 1 \tag{3}$$

In the case of Fig. 2a, we have $U_a = U_{i+}$, so that quantity $\widetilde{U}(x_c, t)$ is the desired estimate of the incident field. For this reason, we call $\widetilde{U}(x_c, t)$ the estimate of the incident field, although this is not true in the case of an incident wave propagating to the left, like in Fig. 2b, since then we have $U_a = U_{t-}$, where U_{t-} is the wave transmitted through the Huygens surface. In the actual implementation of the Huygens ABC, U_a will be the superposition of both kinds of waves.

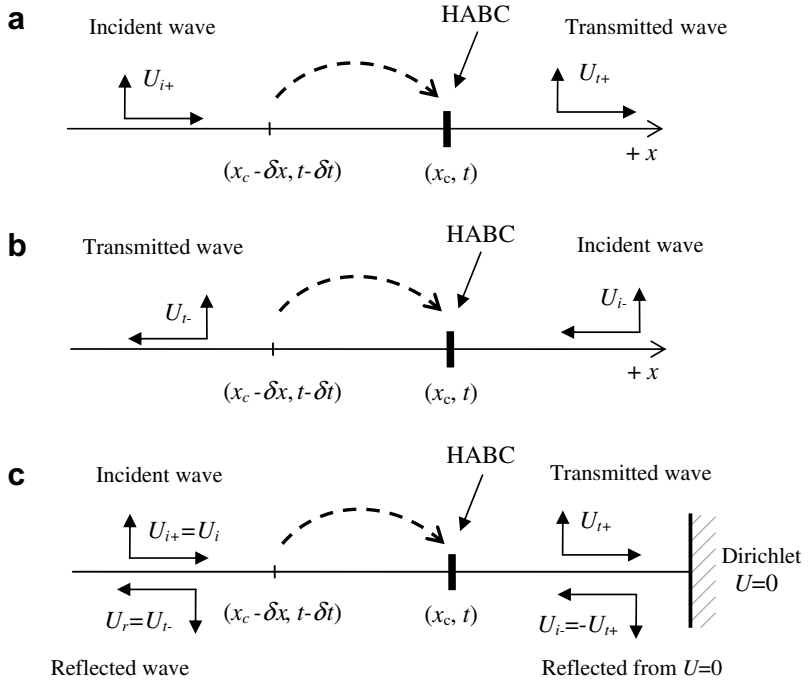

Fig. 2. The Huygens absorbing boundary condition (HABC) in the one-dimensional case.

Let us now define the linear operator

$$P = \sum_{k=1}^{N} a_k K(-\delta x_k) Z(-\delta t_k) \tag{4}$$

where K and Z are shift operators in space and time defined by

$$K(-\delta x)U(x,t) = U(x-\delta x,t) \quad \text{and} \quad Z(-\delta t)U(x,t) = U(x,t-\delta t) \tag{5}$$

Then, estimate (2) can be rewritten as

$$\widetilde{U}(x_c,t) = PU_{\mathrm{a}}(x_c,t) \tag{6}$$

In this paragraph, we only consider the following operator, called the elementary operator:

$$P_{\mathrm{e}} = K(-\delta x)Z(-\delta t) \tag{7}$$

with which (2) becomes

$$\widetilde{U}(x_c,t) = U_{\mathrm{a}}(x_c-\delta x, t-\delta t) \tag{8}$$

The estimate of the incident field at (x_c,t) equals the field that was present at location $x_c-\delta x$ at time $t-\delta t$. Operator (7) was used by Higdon as an absorbing boundary condition in paper [5] where it is called the space–time extrapolation operator.

Consider now the case in Fig. 2a. The field transmitted to the right-hand side of x_c, at an infinitesimal distance from x_c, is the addition of $U_{i+}(x_c,t)$ that would be present in the absence of the Huygens surface, with the field radiated from the Huygens surface, that is the opposite of $\widetilde{U}(x_c,t)$. Denoting as U_{t+} the transmitted field, this reads

$$U_{t+}(x_{c+},t) = U_{i+}(x_c,t_)) - \widetilde{U}(x_c,t) \tag{9}$$

Using (8) and (9), and with $U_{\mathrm{a}} = U_{i+}$, the transmitted field is then

$$U_{t+}(x_{c+},t) = U_{i+}(x_c,t) - U_{i+}(x_c-\delta x, t-\delta t) \tag{10}$$

Assuming now that δx and δt are small, we can write

$$U_{i+}(x_c-\delta x, t-\delta t) = U_{i+}(x_c,t) - \frac{\partial U_{i+}(x_c,t)}{\partial x}\delta x - \frac{\partial U_{i+}(x_c,t)}{\partial t}\delta t \tag{11}$$

with which (10) becomes

$$U_{t+}(x_{c+},t) = \frac{\partial U_{i+}(x_c,t)}{\partial x}\delta x + \frac{\partial U_{i+}(x_c,t)}{\partial t}\delta t \tag{12}$$

Moreover, since the incident field is of the form $U_{i+}(t-x/c)$, we have

$$\frac{\partial U_{i+}(x_c,t)}{\partial x} = -\frac{1}{c}\frac{\partial U_{i+}(x_c,t)}{\partial t} \tag{13}$$

so that (12) can be rewritten as

$$U_{t+}(x_{c+},t) = \left(\delta t - \frac{\delta x}{c}\right)\frac{\partial U_{i+}(x_c,t)}{\partial t}. \tag{14}$$

The transmitted field equals the time derivative of the incident field, multiplied with a coefficient that depends on the space and time distances δx and δt used for estimating the incident field. The above derivation relies on (11). It is rigorous as δx and δt tend to zero.

Consider now the case in Fig. 2b where the incident wave comes from the right-hand side. The incident field is then of the form $U_{i-}(t+x/c)$ and a transmitted field $U_{t-}(t+x/c)$ is present to the left of x_c. Assume that the Huygens surface is left unchanged in comparison with the previous case. The estimate of the impressed field is given by (8) with now $U_{\mathrm{a}} = U_{t-}$. This impressed field propagates to the left, i.e. the source is now to the right of the Huygens surface, so that the sign of the normal in (1) is opposite to its physical orientation. The

Huygens surface acts as an anti-Huygens surface for this impressed field. From this, it will radiate a wave equal to the "opposite of the opposite" of the estimate $\widetilde{U}(x_c,t)$. At an infinitesimal distance to the left of x_c, the transmitted field is then

$$U_{t-}(x_{c-},t) = U_{i-}(x_c,t) + \widetilde{U}(x_c,t) \tag{15}$$

in place of (9). With elementary operator (7), (8), the estimate $\widetilde{U}(x_c,t)$ equals the field at location $x_c-\delta x$ and time $t-\delta t$, that is

$$\widetilde{U}(x_c,t) = U_{t-}(x_{c-}-\delta x, t-\delta t) \tag{16}$$

so that

$$U_{t-}(x_{c-},t) = U_{i-}(x_c,t) + U_{t-}(x_{c-}-\delta x, t-\delta t) \tag{17}$$

Using now

$$U_{t-}(x_{c-}-\delta x, t-\delta t) = U_{t-}(x_{c-},t) - \frac{\partial U_{t-}(x_{c-},t)}{\partial x}\delta x - \frac{\partial U_{t-}(x_{c-},t)}{\partial t}\delta t \tag{18}$$

Eq. (17) becomes

$$\frac{\partial U_{t-}(x_{c-},t)}{\partial x}\delta x + \frac{\partial U_{t-}(x_{c-},t)}{\partial t}\delta t = U_{i-}(x_c,t) \tag{19}$$

Finally, using a relation like (13) with sign + in place of sign – due to the propagation to the left

$$\frac{\partial U_{t-}(x_{c-},t)}{\partial t} = \frac{1}{(\delta t + \delta x/c)} U_{i-}(x_c,t) \tag{20}$$

or equivalently

$$U_{t-}(x_{c-},t) = \frac{1}{(\delta t + \delta x/c)} \int U_{i-}(x_c,t')\,\mathrm{d}t'. \tag{21}$$

Thus, in the case of waves propagating in $-x$ direction the transmitted field equals the integral of the incident field, multiplied with a coefficient.

If we now consider the case in Fig. 2c, where the 1D space is ended with Dirichlet condition $U=0$, that is a perfect electric condition or a perfect magnetic condition in electromagnetics. The wave incident from the left-hand side is transmitted through the HABC according to (14). It is then reflected from $U=0$ condition with reflection coefficient -1, and transmitted back to the left of the Huygens surface according to (21). The overall reflection, i.e. the ratio r of fields U_r and U_i in Fig. 2c, is then

$$r = \frac{\delta x - c\delta t}{\delta x + c\delta t} \tag{22}$$

The reflected wave is a copy of the incident wave, i.e. the Huygens ABC is non dispersive.

Consider now an operator absorbing boundary condition placed at the end of the 1D space, as depicted in Fig. 3. An operator ABC consists of enforcing a value estimated from the field at one or several locations and times in the inner space. Assume that this estimate is given by the elementary operator (7). Then, at location x_b the incident and reflected waves satisfy the following relationship:

$$U_i(x_b,t) + U_r(x_b,t) = U_i(x_b-\delta x, t-\delta t) + U_r(x_b-\delta x, t-\delta t) \tag{23}$$

For small δx and δt, we can write

$$U_i(x_b-\delta x, t-\delta t) = U_i(x_b,t) - \frac{\partial U_i(x_b,t)}{\partial x}\delta x - \frac{\partial U_i(x_b,t)}{\partial t}\delta t \tag{24a}$$

$$U_r(x_b-\delta x, t-\delta t) = U_r(x_b,t) - \frac{\partial U_r(x_b,t)}{\partial x}\delta x - \frac{\partial U_r(x_b,t)}{\partial t}\delta t \tag{24b}$$

where the space derivatives can be replaced with time derivatives, because U_i and U_r are of the form $U_i(t-x/c)$ and $U_r(t+x/c)$, respectively. Inserting then (24a) and (24b) into (23), the following is obtained:

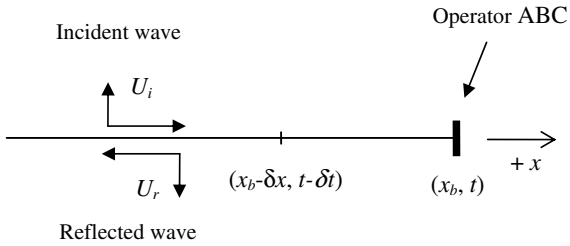

Fig. 3. Operator absorbing boundary condition ending a computational domain.

$$0 = \frac{\partial U_i(x_b,t)}{\partial t}\frac{\delta x}{c} - \frac{\partial U_i(x_b,t)}{\partial t}\delta t - \frac{\partial U_r(x_b,t)}{\partial t}\frac{\delta x}{c} - \frac{\partial U_r(x_b,t)}{\partial t}\delta t \tag{25}$$

Integrating on time, this yields

$$U_i(x_b,t)(\delta x/c - \delta t) = U_r(x_b,t)(\delta x/c + \delta t) \tag{26}$$

From this, ratio $r = U_r/U_i$ is equal to (22). Thus, the reflection from the operator ABC equals, rigorously, the reflection from the Huygens ABC that relies on the same operator for estimating the Huygens currents.

A numerical experiment is reported in Fig. 4. The experiment was performed using the FDTD method. We used shifts equal to the steps of the FDTD scheme, that is $\delta x = \Delta x$ and $\delta t = \Delta t$. The incident wave was the Gaussian pulse

$$E_i(t) = \mathrm{e}^{-\frac{(t-3T)^2}{T^2}} \quad T = 1\ \mathrm{ns} \tag{27}$$

The calculation was performed with a source placed to the left of the Huygens surface, and two observation points were placed on the two sides of the Huygens surface, at A and B locations, respectively. The corresponding FDTD results are compared with theoretical predictions (14) and (22). Fig. 4a shows the incident wave (27) at A, Fig. 4b compares the transmitted wave at B with its prediction (14), Fig. 4c shows the wave

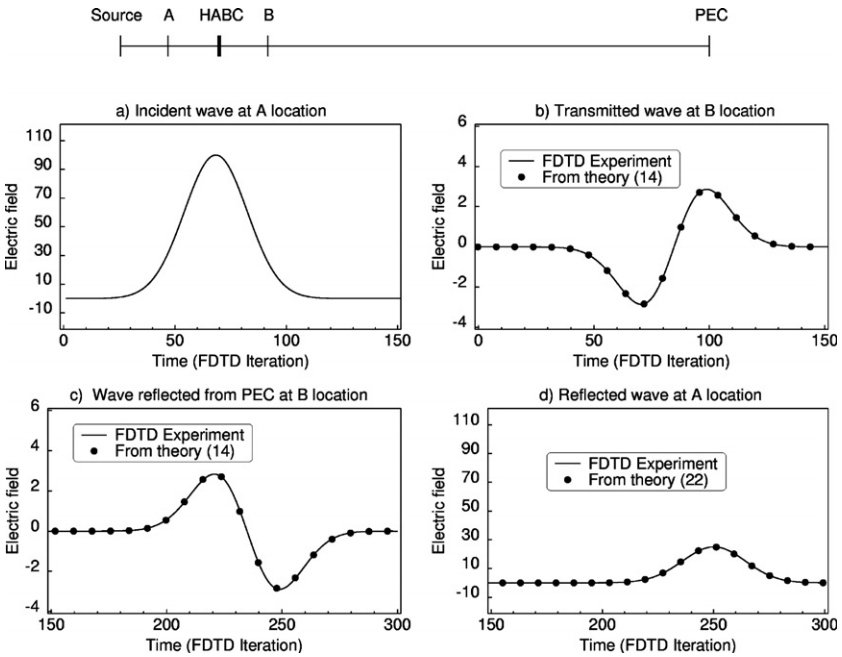

Fig. 4. Transmission through the Huygens surface and reflection from the Huygens ABC. A comparison of theory with FDTD one-dimensional experiment. The FDTD steps are $\Delta x = 5$ cm and $\Delta t = 100$ ps. The wave is observed at A and B locations on the two sides of the HABC. The distances from the source to A, HABC, B and PEC are 5, 10, 15 and 60 FDTD cells, respectively.

reflected from the PEC condition at B, and Fig. 4d compares the overall reflected wave at A with its prediction (22). As observed, the FDTD results are in a quite good accordance with (14) and (22). Especially, the wave at B location is the derivative of the incident wave (27). This wave is then integrated in time as passing back through the Huygens surface so that it becomes a copy of the incident wave (27) multiplied with coefficient (22). An additional calculation was performed with the HABC replaced with the operator ABC at the end of the domain. As expected the reflection observed at A location was superimposed to that from the HABC. In conclusion, the FDTD experiments are in a good accordance with predictions derived in continuous spaces. This suggests that (14) and (21) are also valid in the FDTD discretized space. This will be proved theoretically later in this paper.

3.2. Derivation using single frequency waveforms

If in place of waves of the form $U(t - x/c)$ we consider single frequency waves we also find the same conclusions as in the above. For the direct transmission in Fig. 2a and an incident wave $\exp(j\omega t - j\omega x/c)$, where ω is the angular frequency, the following replaces (11):

$$U_{i+}(x_c - \delta x, t - \delta t) = U_{i+}(x_c, t)e^{-j\omega\delta t}e^{j\omega\delta x/c} \tag{28}$$

Substituting then (28) into (10) yields

$$U_{t+}(x_{c+}, t) = U_{i+}(x_c, t)[1 - e^{-j\omega\delta t}e^{j\omega\delta x/c}] \tag{29}$$

In the case where $\omega\delta t \ll 1$ and $\omega\delta x/c \ll 1$ that corresponds to δt small vs. the period of the wave, and δx small vs. the wavelength, using the first-order expansion of the exponentials, (29) becomes

$$U_{t+}(x_{c+}, t) = j\omega\left(\delta t - \frac{\delta x}{c}\right)U_{i+}(x_c, t) \tag{30}$$

that is consistent with (14) because a multiplication with $j\omega$ in frequency domain is a time derivative in time-domain. Similarly, for the reverse transmission in Fig. 2b, the equivalent of (21) can be obtained where the integral in (21) is replaced with $U_{i-}(x_c, t)/j\omega$. This also yields the overall reflection coefficient (22).

3.3. Generalization to 2D and 3D cases

The above derivations can be generalized easily to 2D and 3D spaces. In those cases, assume that the direction of propagation forms an angle θ with respect to direction x. The waveforms are then $U(t - x\cos\theta/c)$ or $U(t + x\cos\theta/c)$, so that celerity c is replaced with $c/\cos\theta$ in the derivations, especially in (14), (21) and (23). The overall reflection from the HABC, and the reflection from the elementary operator ABC, are then

$$r = \frac{\cos\theta\delta x - c\delta t}{\cos\theta\delta x + c\delta t} \tag{31}$$

3.4. The Huygens ABC with general operators

In the above the elementary operator (7) has been used for the estimation of the incident wave at the Huygens surface location. All the derivations can be reproduced with general operator (4) that is a linear combination of elementary operators, with coefficients satisfying (3).

For the case in Fig. 2a where the incident wave propagates to the right, (2) and (9) yield

$$U_{t+}(x_{c+}, t) = U_{i+}(x_c, t) - \sum_{k=1}^{N} a_k U_{i+}(x_c - \delta x_k, t - \delta t_k) \tag{32}$$

With expansions like (11), this can be rewritten as

$$U_{t+}(x_{c+}, t) = U_{i+}(x_c, t) - \sum_{k=1}^{N} a_k U_{i+}(x_c, t) + \sum_{k=1}^{N} a_k\left(\frac{\partial U_{i+}(x_c, t)}{\partial x}\delta x_k + \frac{\partial U_{i+}(x_c, t)}{\partial t}\delta t_k\right) \tag{33}$$

Using then (3) and (13), the following transmitted field is obtained in the 2D and 3D cases where the incident wave forms an angle θ with x direction:

$$U_{t+}(x_{c+},t)=\frac{\partial U_{i+}(x_c,t)}{\partial t}\sum_{k=1}^{N}a_k\left(\delta t_k-\frac{\cos\theta\delta x_k}{c}\right) \tag{34}$$

This shows that the transmitted wave is the derivative of the incident wave with any operator (4) used for estimating the incident wave at the Huygens surface location. In the case of Fig. 2b where the wave propagates to the left, (2) and (15) yield

$$U_{t-}(x_{c-},t)=U_{i-}(x_c,t)+\sum_{k=1}^{N}a_kU_{t-}(x_{c-}-\delta x_k,t-\delta t_k) \tag{35}$$

Proceeding as in the above, the following transmitted wave is obtained, in place of (21):

$$U_{t-}(x_{c-},t)=\frac{1}{\sum_{k=1}^{N}a_k(\delta t_k+\cos\theta\delta x_k/c)}\int U_{i-}(x_c,t')\,\mathrm{d}t' \tag{36}$$

From this, the overall reflection for the space bounded with a Dirichlet condition, like in Fig. 2c is

$$r=\frac{\sum_{k=1}^{N}a_k(\cos\theta\delta x_k-c\delta t_k)}{\sum_{k=1}^{N}a_k(\cos\theta\delta x_k+c\delta t_k)} \tag{37}$$

Generalization of derivations (23)–(26) easily shows that (37) is also the reflection from operator (4) used as a boundary condition. Thus, with (2)–(4) the wave radiated from the HABC is the derivative of the outgoing wave, the wave reflected from the outer boundary is integrated as it passes back through the HABC, and the overall reflection is equal, rigorously, to the reflection from the corresponding operator ABC. Strictly speaking, this clearly demonstrates that Huygens ABCs are not novel ABCs. They are only alternative implementations of previously used operator ABCs.

The derivations and conclusions in the above may be slightly changed with some special cases of operator (4). This arises when the first-order terms of the expansion (33) vanish. As shown in Appendix A, in that case the first derivative in (34) is replaced with the second derivative, and the integral in (36) is replaced with a double integral on time. The coefficients in (34) and (36) are also modified, so that the overall reflection (37) is no longer valid. The right reflection that replaces (37) is given in Appendix A.

3.5. The Higdon operators

The Higdon operators [5,6] are an important class of operators used as absorbing boundary conditions. Obviously they can also be used to obtain the estimate of the incident field at the Huygens ABC. The Higdon boundary condition considered in [6] can be written as

$$\left[\prod_{j=1}^{p}(I-P_{\mathrm{H1}}(\theta_j))\right]U(x_b,t)=0 \tag{39}$$

where I is the identity operator and

$$P_{\mathrm{H1}}(\theta_j)=K(-\Delta x)Z(-\Delta t)+w(\theta_j)K(-\Delta x)-w(\theta_j)Z(-\Delta t) \tag{40a}$$

with

$$w(\theta_j)=\frac{c\Delta t-\cos\theta_j\Delta x}{c\Delta t+\cos\theta_j\Delta x} \tag{40b}$$

where Δx and Δt are the space and time steps of the finite method, and θ_j angles are the incidences where the reflection vanishes. Boundary condition (39) can be rewritten as

$$(I-P_{\mathrm{H}p})U(x_b,t)=0 \tag{41}$$

with

$$P_{\mathrm{H}p} = I - \prod_{j=1}^{p}(I - P_{\mathrm{H1}}(\theta_j)) \tag{42}$$

In the following, $P_{\mathrm{H}p}$ is called the p-order Higdon operator.

The first term of the first-order Higdon operator P_{H1} (40a) is the elementary operator (7). Its second term is also (7) in the special case $\delta t = 0$. But its third term $wZ(-\Delta t)$ is not a special case $\delta x = 0$ of (7), because (4) has been defined for $\delta x > 0$, in accordance with the fact that the incident field cannot be known at the Huygens surface location. So, strictly speaking, Higdon operator (40a) is not a special case of general operator (4). Like using it as an operator ABC [6], in actual implementation of (40a) the term $wZ(-\Delta t)$ is applied to the estimate $\widetilde{U}(x_c, t)$ in place of the exact field $U(x_c, t)$. It is proved in Appendix B that this replacement left unchanged the overall reflection from the HABC. It is given by (37) with a_k coefficients in (40a). This also holds with any operator (4). If $\delta x_k = 0$ for one or several terms in (4), reflection (37) is still valid. From this, we can consider that the domain of definition of operator (4) can be extended to $\delta x \geqslant 0$, with U replaced with $\widetilde{U}$ in the case $\delta x = 0$.

From (42) the second-order operator reads

$$P_{\mathrm{H2}} = P_{\mathrm{H1}}(\theta_1) + P_{\mathrm{H1}}(\theta_2) - P_{\mathrm{H1}}(\theta_1)P_{\mathrm{H1}}(\theta_2) \tag{43}$$

Using (40a), and with $K(-\Delta x)K(-\Delta x) = K(-2\Delta x)$ and $Z(-\Delta t)Z(-\Delta t) = Z(-2\Delta t)$, the following second-order Higdon operator is obtained:

$$\begin{aligned} P_{\mathrm{H2}} = {} & (w_1 + w_2)K(-\Delta x) - w_1 w_2 K(-2\Delta x) - (w_1 + w_2)Z(-\Delta t) + 2(1 + w_1 w_2)K(-\Delta x)Z(-\Delta t) \\ & - (w_1 + w_2)K(-2\Delta x)Z(-\Delta t) - w_1 w_2 Z(-2\Delta t) + (w_1 + w_2)K(-\Delta x)Z(-2\Delta t) - K(-2\Delta x)Z(-2\Delta t) \end{aligned} \tag{44}$$

where $w_1 = w(\theta_1)$ and $w_2 = w(\theta_2)$. Notice that (3) holds with coefficients in (44). Like (40a), (44) is an operator (4) with the extension of its definition to $\delta x = 0$. Finally, since (40a) and (44) are special cases of (4), using the Higdon operators to estimate the incident wave to be impressed at the Huygens surface of the Huygens ABC, the overall reflection is equal to the reflection from the corresponding Higdon operator used as an absorbing boundary condition (39). This is also true with any p-order Higdon operator (42). This will be confirmed by means of numerical experiments with the FDTD method in the next section.

3.6. The Huygens ABC with evanescent waves

In previous section, only traveling waves have been addressed, that is waves whose magnitude is constant in the direction perpendicular to the direction of propagation. Unfortunately, this is not sufficient, because in most problems of numerical electromagnetics evanescent waves are present. It can be shown that general plane wave solutions of the Maxwell equations are as follows, where U is any component of the field

$$U = U_0 \mathrm{e}^{\mathrm{j}\omega\left[t - \frac{\cosh\chi}{c}(x\cos\theta + y\sin\theta)\right]} \mathrm{e}^{-\frac{\omega}{c}\sinh\chi(y\cos\theta - x\sin\theta)} \tag{45}$$

where $-\pi < \theta < \pi$ and $-\infty < \chi < \infty$. The phase propagates in direction θ with respect to x, and the magnitude decreases in the direction perpendicular to θ. With (45), we can write, in place of (11) or (28)

$$U_{i+}(x_c - \delta x, t - \delta t) = U_{i+}(x_c, t)\mathrm{e}^{-\mathrm{j}\omega\delta t}\mathrm{e}^{\mathrm{j}\omega\frac{\cosh\chi\cos\theta}{c}\delta x}\mathrm{e}^{-\frac{\omega}{c}\sinh\chi\sin\theta\delta x} \tag{46}$$

Substituting then (46) into (10) the following transmitted wave is obtained

$$U_{t+}(x_{c+}, t) = U_{i+}(x_c, t)\left[1 - \mathrm{e}^{-\mathrm{j}\omega\delta t}\mathrm{e}^{\mathrm{j}\omega\frac{\cosh\chi\cos\theta}{c}\delta x}\mathrm{e}^{-\frac{\omega}{c}\sinh\chi\sin\theta\delta x}\right] \tag{47}$$

In view of the application to finite methods, where δx and δt will be the space and time steps, we can assume that $\omega\delta t \ll 1$, as with traveling waves, and that $\omega|\sinh\chi|\delta x/c \ll 1$, in order that the evanescent waves be accurately sampled. From this, (47) becomes

$$U_{t+}(x_{c+},t)=\left[\mathrm{j}\omega\left(\delta t-\cosh\chi\cos\theta\frac{\delta x}{c}\right)+\frac{\omega}{c}\sinh\chi\sin\theta\delta x\right]U_{i+}(x_c,t) \tag{48}$$

that holds as a special case the traveling wave case ($\cosh\chi=1$ and $\sinh\chi=0$). In the general case, the field outside the Huygens surface is not the derivative of the incident field, an additional term proportional to the incident wave is present, due to the real term in the bracket in (48).

It is known that coefficients θ and χ of evanescent waves reflected from a PEC or any interface are changed to $\pi-\theta$ and $-\chi$, respectively, so that the wave reflected from the Dirichlet condition ending the HABC is of the form

$$U=U_0\mathrm{e}^{\mathrm{j}\omega\left[t-\frac{\cosh\chi}{c}(-x\cos\theta+y\sin\theta)\right]}\mathrm{e}^{+\frac{\omega}{c}\sinh\chi(-y\cos\theta-x\sin\theta)} \tag{49}$$

Using this in (17), the following transmission is obtained, in place of (21):

$$U_{t-}(x_{c-},t)=\frac{1}{\mathrm{j}\omega\left(\delta t+\cosh\chi\cos\theta\frac{\delta x}{c}\right)-\frac{\omega}{c}\sinh\chi\sin\theta\delta x}U_{i-}(x_c,t) \tag{50}$$

Finally, taking account of reflection -1 from the Dirichlet condition, the overall reflection coefficient of the evanescent wave from the HABC is

$$r=\frac{\mathrm{j}(\cosh\chi\cos\theta\delta x-c\delta t)-\sinh\chi\sin\theta\delta x}{\mathrm{j}(\cosh\chi\cos\theta\delta x+c\delta t)-\sinh\chi\sin\theta\delta x} \tag{51}$$

The above derivation can be generalized to the general operator (2)–(4). This yields

$$r=\frac{\sum_{k=1}^{N}a_k[\mathrm{j}(\cosh\chi\cos\theta\delta x_k-c\delta t_k)-\sinh\chi\sin\theta\delta x_k]}{\sum_{k=1}^{N}a_k[\mathrm{j}(\cosh\chi\cos\theta\delta x_k+c\delta t_k)-\sinh\chi\sin\theta\delta x_k]} \tag{52}$$

It could be shown easily that (52) is also the reflection from the operator used as an operator ABC. Obviously, (51) and (52) reduce to (31) and (37) in the case of traveling waves ($\sinh\chi=0$ and $\cosh\chi=1$). Various special cases can be found from (51) and (52). In the case of strongly evanescent waves ($\cosh\gg 1$), we have

$$r(\cosh\chi\gg 1)=1 \tag{53}$$

The reflection of strongly evanescent waves is total from the HABC with any operator (4), especially with Higdon operators. Then, the HABC suffers from the same drawback as the Higdon operator ABC, it cannot absorb evanescent waves that are present in most problems of practical interest in numerical electromagnetics. This will be confirmed by numerical experiments in the following. Another special case is when $\theta=\pm\pi/2$. The wave is evanescent in x-direction and the phase varies in direction perpendicular to x. The reflection is then

$$r=-\frac{\sum_{k=1}^{N}a_k[\mathrm{j}c\delta t_k\pm\sinh\chi\delta x_k]}{\sum_{k=1}^{N}a_k[\mathrm{j}c\delta t_k\mp\sinh\chi\delta x_k]} \tag{54}$$

whose modulus equals unity (ratio of complex conjugates). In the case of traveling waves ($\sinh\chi=0$) we have $r=-1$. This is consistent with the phase propagation in direction parallel to the boundary (incidence $\theta=\pm\pi/2$). In the case of strongly evanescent waves, i.e. if $|\sinh\chi|\gg 1$, we have $r=1$, in accordance with (53).

Numerical experiments have been performed with the FDTD method in a 2D case involving both traveling and evanescent waves. The problem is depicted in Fig. 5. The first transverse magnetic (TM_1) mode is impressed in a parallel plate waveguide. For this mode, above cut-off frequency

$$\omega_c=\frac{\pi c}{a} \tag{55}$$

the field is of the form

$$H_z(x,y,t)=H_0\mathrm{e}^{\mathrm{j}\omega t}\left(\mathrm{e}^{-\mathrm{j}\frac{\omega}{c}\sin\theta y}+\mathrm{e}^{\mathrm{j}\frac{\omega}{c}\sin\theta y}\right)\mathrm{e}^{-\mathrm{j}\frac{\omega}{c}\cos\theta x} \tag{56a}$$

where $\sin\theta=\omega_c/\omega$. This field is the sum of two traveling waves propagating in directions $\pm\theta$. Below cut-off (55), the field is the addition of two evanescent waves

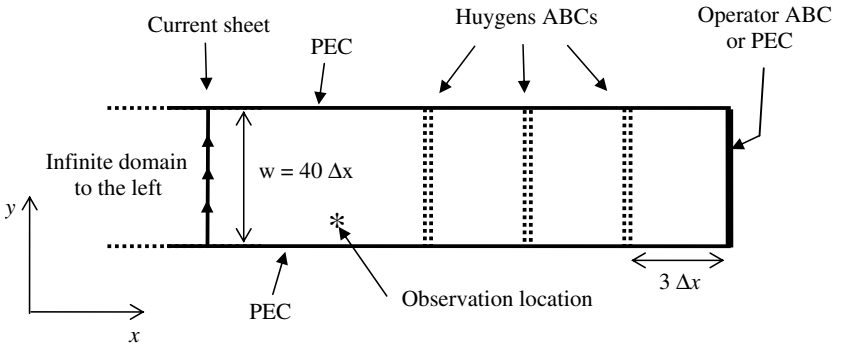

Fig. 5. Parallel plate waveguide. The space steps are $\Delta x = \Delta y = 1$ mm, with $\Delta t = 1.666$ ps. The TM_1 mode is generated with a current sheet $\sin(\pi(y - w/2)/w)$ where w is the guide width (40 mm) and $0 < y < w$. The domain is large enough to the left so that the reflection from its end is not viewed during computation. One or several HABCs are placed to the right of the observation point. The domain is ended either with a PEC condition or with an operator ABC. The figure is not to scale, the guide width is $w = 40\ \Delta y = 40$ mm, the ABC separations are $3\Delta x = 3$ mm.

$$H_z(x,y,t) = H_0\left(e^{-j\frac{\omega}{c}\cosh\chi y} + e^{j\frac{\omega}{c}\cosh\chi y}\right)e^{-\frac{\omega}{c}\sinh\chi x} \tag{56b}$$

where $\cosh\chi = \omega_c/\omega$ and $\sinh\chi > 0$. These waves are special cases of (45) with $\theta \pm \pi/2$ and $\theta\chi < 0$.

Calculations were performed either with a Huygens ABC, an operator ABC, or with both conditions. A reference solution was computed with a large waveguide in order that the reflection from its end was not viewed during the calculation. The field was recorded some cells in front of the HABC and the reflected field was obtained by subtracting the reference field. The calculations were performed with a pulse. Results in frequency domain were computed by means of a Fourier transform.

Fig. 6 shows comparisons of reflection from a Huygens ABC (HABC) with reflection from the corresponding operator ABC (OABC). In both cases the operators are either a first-order or a second-order Higdon operator. In addition, the reflection without ABC, computed with a PEC ending the domain, is reported. As observed, reflections from the HABC and from the OABC are identical, provided that they rely on the same operator. This is true in the traveling wave region, where the Higdon ABCs are effective, and in the evanescent region where the Higdon operators do not absorb the field. The small attenuation in this region, about 6 dB, is only due to the natural decay of the evanescent waves. So, this experiment confirms what has been derived theoretically. The HABC is equivalent, rigorously, to the operator ABC relying on the same operator. Especially, using such operators as the Higdon operators that reflect in totality evanescent fields, the HABC also reflects in totality evanescent fields.

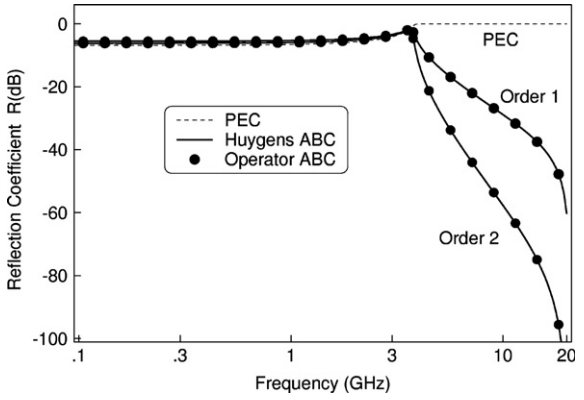

Fig. 6. Comparison of the reflection coefficients computed using either an operator ABC at the end of the waveguide or a Huygens ABC in conjunction with a PEC ending the waveguide. In both cases the operators are either the first-order Higdon operator (40) or the second-order Higdon operator (44). The reflection coefficients are expressed in decibels (dB), i.e. $R(\text{dB}) = 20\log_{10}(R)$.

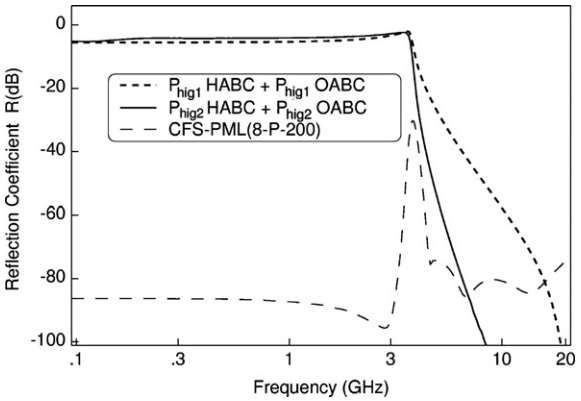

Fig. 7. Reflection from the end of the waveguide using a Huygens ABC (HABC) in conjunction with an operator ABC (OABC). In both ABCs the operators are Higdon operators.

Fig. 7 shows reflections computed using combinations of the HABC with the OABC. In the first case the first-order Higdon operator is used with both the HABC and the OABC. As expected the reflection is identical to that obtained with the second-order operator impressed either as a HABC or as an OABC (Fig. 6). In the second experiment, the second-order Higdon operator is used, so that the set HABC + OABC is equivalent to a fourth-order Higdon ABC. As observed, the reflection of traveling waves is then quite small. But such a high-order operator remains ineffective for the absorption of evanescent waves. The reflection is total, in contrast to the reflection from a PML that may be quite small, as illustrated with the result reported in the figure. The PML is the optimized CFS-PML eight cells in thickness used in [8].

4. The Huygens ABC in the discretized space of the FDTD method

In previous section, the reflection from the HABC has been addressed in continuous spaces. As known, in numerical methods the field radiated from Huygens surfaces slightly differ from its theoretical value. Nevertheless, the reported numerical experiments have shown a very good agreement of the FDTD method with predictions in continuous spaces, especially in Fig. 4. This suggests that the properties of the continuous HABC are preserved in the FDTD discretized space. This is confirmed theoretically in the following by deriving the FDTD counterparts of transmissions (14), (21) and reflection (22).

We consider the 1D case whose FDTD grid is depicted in Fig. 8. We assume that an incident wave with components E_y and H_z propagates in $+x$ direction. The Huygens surface is placed between nodes $E_y(0)$ and $H_z(1/2)$. Using (1) the equivalent currents at these nodes, at times $n+1/2$ and n, are

$$J_{Sy}^{n+1/2}(0) = -\widetilde{H}_z^{n+1/2}(1/2) \quad \text{and} \quad K_{Sz}^{n}(1/2) = -\widetilde{E}_y^{n}(0) \tag{57}$$

where $\widetilde{E}_y$ and $\widetilde{H}_z$ are the estimates of the incident components. Using the elementary operator (7), with δx and δt equal to the space and time steps of the FDTD grid, the estimates read

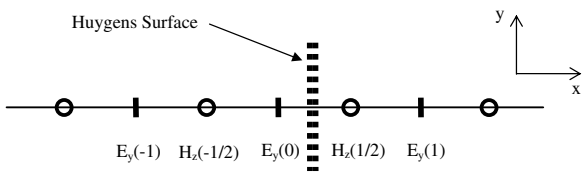

Fig. 8. Implementation of the Huygens surface in the one-dimensional FDTD grid.

$$\widetilde{H}_z^{n+1/2}(1/2) = H_z^{n-1/2}(-1/2) \quad \text{and} \quad \widetilde{E}_y^n(0) = E_y^{n-1}(-1) \tag{58}$$

Introducing the opposite of surface current densities (57) into the FDTD equations, the following set is obtained for the advance of the field at nodes $E_y(0)$ and $H_z(1/2)$

$$E_y^{n+1}(0) = E_y^n(0) - \frac{\Delta t}{\varepsilon_0 \Delta x}[H_z^{n+1/2}(1/2) - H_z^{n+1/2}(-1/2)] - \frac{\Delta t}{\varepsilon_0 \Delta x} H_z^{n-1/2}(-1/2) \tag{59a}$$

$$H_z^{n+1/2}(1/2) = H_z^{n-1/2}(1/2) - \frac{\Delta t}{\mu_0 \Delta x}[E_y^n(1) - E_y^n(0)] - \frac{\Delta t}{\mu_0 \Delta x} E_y^{n-1}(-1) \tag{59b}$$

Notice that (59a) and (59b) are consistent with the fact that $E_y(0)$ is in the incident field region and $H_z(1/2)$ is in the total field region (incident field plus radiated field). For instance, (59a) can be interpreted as the regular FDTD equation at node $E_y(0)$, in the incident region, because the additional term $H_z^{n-1/2}(-1/2)$ subtracts the radiated field to the total field $H_z^{n+1/2}(1/2)$.

For a given incident wave propagating to the right, we assume that there are a transmitted wave propagating to the right and a reflected wave propagating to the left. We assume in addition that the space and time dependences of E_y are of the form

$$E_{yi} = E_{i0} e^{j\omega t - jk_x x} \tag{60a}$$

$$E_{yr} = E_{r0} e^{j\omega t + jk_x x} \tag{60b}$$

$$E_{yt} = E_{t0} e^{j\omega t - jk_x x} \tag{60c}$$

where k_x is the wave number in the FDTD discretized space. It is known [4] that the impedance in a FDTD grid is like in the continuous space, so that the same dependences also hold for H_z fields, with magnitudes $H_{i0} = E_{i0}/Z_0$, $H_{r0} = -E_{r0}/Z_0$, $H_{t0} = E_{t0}/Z_0$, where $Z_0 = \sqrt{\mu_0/\varepsilon_0}$. Enforcing (60) into (59) yields

$$\begin{aligned}(E_{i0} + E_{r0}) e^{j\omega\Delta t} = E_{i0} + E_{r0} - \frac{\Delta t}{\varepsilon_0 \Delta x}\left[\frac{E_{t0}}{Z_0} e^{j\omega\Delta t/2} - \frac{E_{i0}}{Z_0} e^{j\omega\Delta t/2} e^{jk_x\Delta x/2} + \frac{E_{r0}}{Z_0} e^{j\omega\Delta t/2} e^{-jk_x\Delta x/2}\right] \\ - \frac{\Delta t}{\varepsilon_0 \Delta x}\left[\frac{E_{i0}}{Z_0} e^{-j\omega\Delta t/2} e^{jk_x\Delta x/2} - \frac{E_{r0}}{Z_0} e^{-j\omega\Delta t/2} e^{-jk_x\Delta x/2}\right]\end{aligned} \tag{61a}$$

$$\frac{E_{t0}}{Z_0} e^{j\omega\Delta t/2} = \frac{E_{t0}}{Z_0} e^{-j\omega\Delta t/2} - \frac{\Delta t}{\mu_0 \Delta x}[E_{t0} e^{-jk_x\Delta x/2} - (E_{i0} + E_{r0})] - \frac{\Delta t}{\mu_0 \Delta x}[E_{i0} e^{-j\omega\Delta t} e^{jk_x\Delta x} + E_{r0} e^{-j\omega\Delta t} e^{-jk_x\Delta x}] \tag{61b}$$

Denoting as α the quantity

$$\alpha = \frac{c\Delta t}{\Delta x} = \frac{1}{Z_0}\frac{\Delta t}{\varepsilon_0 \Delta x} = Z_0 \frac{\Delta t}{\mu_0 \Delta x} \tag{62}$$

system (61) for unknowns E_{r0} and E_{t0} can be rewritten as

$$AE_{r0} + \alpha E_{t0} = C \tag{63a}$$

$$UE_{t0} + VE_{r0} = W \tag{63b}$$

where

$$A = 2j\sin(\omega\Delta t/2) + \alpha e^{-jk_x\Delta x/2}(1 - e^{-j\omega\Delta t}) \tag{64a}$$

$$C = [-2j\sin(\omega\Delta t/2) + \alpha e^{jk_x\Delta x/2}(1 - e^{-j\omega\Delta t})]E_{i0} \tag{64b}$$

$$U = 2j\sin(\omega\Delta t/2) + \alpha e^{-jk_x\Delta x/2} \tag{64c}$$

$$V = -\alpha + \alpha e^{-jk_x\Delta x} e^{-j\omega\Delta t} \tag{64d}$$

$$W = [\alpha - \alpha e^{jk_x\Delta x} e^{-j\omega\Delta t}]E_{i0} \tag{64e}$$

If we now assume that the frequency is far from the cut-off frequency of the FDTD grid, that is $\omega\Delta t \ll 1$ and $k_x\Delta x \ll 1$, using the first-order expansions of exponentials in (64) yields

$$A = \mathrm{j}\omega\Delta t(1+\alpha) \tag{65a}$$
$$C = \mathrm{j}\omega\Delta t(\alpha-1)E_{i0} \tag{65b}$$
$$U = \alpha \tag{65c}$$
$$V = -\mathrm{j}\alpha(k_x\Delta x + \omega\Delta t) \tag{65d}$$
$$W = \mathrm{j}\alpha(\omega\Delta t - k_x\Delta x)E_{i0} \tag{65e}$$

Solving (63) for unknown E_{t0} and using (65), the following is obtained:

$$E_{t0} = -\mathrm{j}\omega\Delta t\frac{2\alpha\omega\Delta t - 2k_x\Delta x}{-\alpha k_x\Delta x - \omega\Delta t - 2\alpha\omega\Delta t}E_{i0} \tag{66}$$

Using then $\alpha = c\Delta t/\Delta x$ and $\omega = c\ k_x$ that holds in the FDTD space far from the mesh cut-off, after some manipulations the transmitted field (66) becomes

$$E_{t0} = \mathrm{j}\omega\left(\Delta t - \frac{\Delta x}{c}\right)E_{i0} \tag{67}$$

Similarly, solving (63) for E_{r0} the following reflected field is obtained:

$$E_{r0} = \frac{\omega\Delta t - \omega\Delta x/c - \omega\Delta t + \omega\Delta x/c}{-\omega\Delta x/c - \omega\Delta t}E_{i0} = 0 \tag{68}$$

Eq. (67) is identical to (30) and is consistent with (14). In the FDTD space, the wave transmitted through the Huygens surface is also the derivative of the incident wave, multiplied with the same coefficient as in continuous spaces. And from (68) the Huygens surface does not reflect the incident wave. However, we should remember that (67) and (68) are first-order expansions, valid far from the cut-off of the FDTD grid. In actual computations, the Huygens surface will radiate a small field back to the inner domain, as it always arises in FDTD calculation with Huygens surfaces.

Let us now consider an incident wave propagating to the left, as in Fig. 2b. Enforcing in (59) waveforms like (60) with opposite signs in the exponentials on k_x, and with $H_{i0} = -E_{i0}/Z_0$, $H_{r0} = E_{r0}/Z_0$, $H_{t0} = -E_{t0}/Z_0$, the following system is obtained in place of (61):

$$E_{t0}\mathrm{e}^{\mathrm{j}\omega\Delta t} = E_{t0} - \frac{\Delta t}{\varepsilon_0\Delta x}\left[\frac{-E_{i0}+E_{r0}}{Z_0}\mathrm{e}^{\mathrm{j}\omega\Delta t/2} + \frac{E_{t0}}{Z_0}\mathrm{e}^{\mathrm{j}\omega\Delta t/2}\mathrm{e}^{-\mathrm{j}k_x\Delta x/2}\right] - \frac{\Delta t}{\varepsilon_0\Delta x}\frac{-E_{t0}}{Z_0}\mathrm{e}^{-\mathrm{j}\omega\Delta t/2}\mathrm{e}^{-\mathrm{j}k_x\Delta x/2} \tag{69a}$$

$$\frac{-E_{i0}+E_{r0}}{Z_0}\mathrm{e}^{\mathrm{j}\omega\Delta t/2} = \frac{-E_{i0}+E_{r0}}{Z_0}\mathrm{e}^{-\mathrm{j}\omega\Delta t/2} - \frac{\Delta t}{\mu_0\Delta x}\left[E_{i0}\mathrm{e}^{\mathrm{j}k_x\Delta x/2} + E_{r0}\mathrm{e}^{-\mathrm{j}k_x\Delta x/2} - E_{t0}\right] - \frac{\Delta t}{\mu_0\Delta x}E_{t0}\mathrm{e}^{-\mathrm{j}\omega\Delta t}\mathrm{e}^{-\mathrm{j}k_x\Delta x} \tag{69b}$$

By means of a derivation similar to the previous one, assuming again that $\omega\Delta t \ll 1$ and $k_x\Delta x \ll 1$, the following transmitted field is obtained:

$$E_{t0} = \frac{1}{\mathrm{j}\omega(\Delta t + \frac{\Delta x}{c})}E_{i0} \tag{70}$$

which is consistent with the transmitted field found in the continuous case (21). The derivation also shows that the reflected field is zero.

In summary, in the FDTD discretized space the transmitted waves are like in continuous spaces. For an incident wave reflected back to the inner domain, like in Fig. 2c, from (68) and (70) the overall reflection is also given by (22). It could be easily shown that the reflection from the operator ABC based on the elementary operator is also equal to (22) in the FDTD space. So, with the FDTD method the overall reflection from the Huygens ABC equals, rigorously, the reflection from the corresponding operator ABC. This has been derived in the case of the elementary operator (7). This also holds with general operators (4) that are linear combinations of elementary operators, and in 2D or 3D FDTD grids as well.

5. Two applications of the Huygens absorbing boundary conditions

As derived in the above, Huygens ABCs are equivalent to operator ABCs so that they cannot be viewed as novel ABCs. However, the interest of HABCs is larger than that of operator ABCs, because a HABC can be

easily combined with other HABCs or with any other ABC. In the following we present two applications of the HABCs for the solution of problems that could not be addressed using operator ABCs. In the first case operators designed to absorb evanescent waves are combined with operators designed to absorb traveling waves. In the latter case an HABC is combined with the PML ABC.

5.1. Huygens ABC for the absorption of both traveling and evanescent waves at the end of waveguides

Operator ABCs proposed in the literature [5,6,11] cannot deal properly with evanescent waves, because they were designed to absorb waves whose magnitude does not depend on space coordinates. Nevertheless, in some special problems, operators suited to the absorption of evanescent waves can be easily found. This is the case at the end of waveguides, where the phase is constant and the magnitude is evanescent in longitudinal direction x (56b). This permits the field on the boundary to be extrapolated from the field in the inner domain. In mathematical terms, let us consider the operator

$$P_{\text{eva1}} = \beta K(-\delta x) \tag{71}$$

where $0 < \beta \leqslant 1$. In the case of Fig. 2a, using this operator in place of (4) the estimate of the field at Huygens ABC location reads

$$\widetilde{U}(x_c, t) = \beta U_{i+}(x_c - \delta x, t) \tag{72}$$

that yields, for an incident wave of the form (56b)

$$\widetilde{U}(x_c, t) = \beta U_{i+}(x_c, t) \mathrm{e}^{\frac{\omega}{c} \sinh \chi \delta x} \tag{73}$$

Using this estimate in (9) the transmitted field is then

$$U_{t+}(x_{c+}, t) = (1 - \beta \mathrm{e}^{\frac{\omega}{c} \sinh \chi \delta x}) U_{i+}(x_c, t) \tag{74}$$

Similarly, for the wave reflected from the Dirichlet condition, the following counterpart of (21) is obtained:

$$U_{t-}(x_{c-}, t) = \frac{1}{1 - \beta \mathrm{e}^{-\frac{\omega}{c} \sinh \chi \delta x}} U_{i-}(x_c, t) \tag{75}$$

so that the overall reflection from the HABC is

$$r = -\frac{1 - \beta \mathrm{e}^{\frac{\omega}{c} \sinh \chi \delta x}}{1 - \beta \mathrm{e}^{-\frac{\omega}{c} \sinh \chi \delta x}} \tag{76}$$

This reflection vanishes, provided that

$$\beta = \mathrm{e}^{-\frac{\omega}{c} \sinh \chi \delta x} \tag{77}$$

This condition only holds for a single frequency. In the case of a waveguide mode, like the TM_1 mode, we have $\cosh \chi = \omega_c/\omega$, so that

$$\omega^2 \sinh^2 \chi = \omega_c^2 - \omega^2 \tag{78}$$

that reduces to $\omega \sinh \chi = \omega_c$ far below cut-off (55). Using this and (55), (77) becomes

$$\beta = \mathrm{e}^{-\frac{\pi}{a} \delta x} \tag{79}$$

With operator (71) and β from (79), the low frequency evanescent waves are totally absorbed by the HABC. It can be easily shown that (76) is also the reflection coefficient using (71) as an operator ABC on the boundary of the domain. By cascading (71) like the first-order Higdon operator (42), the following second-order operator is obtained:

$$P_{\text{eva2}} = \beta_1 K(-\delta x) + \beta_2 K(-\delta x) - \beta_1 \beta_2 K(-2\delta x) \tag{80}$$

whose reflection is the product of two coefficients (76) with β replaced with β_1 and β_2.

Fig. 9 shows results of experiments with the waveguide in Fig. 5 and operators (71) and (80). The reflection was computed using (71) and (80) either with the HABC or as an operator ABC. As expected, once again the

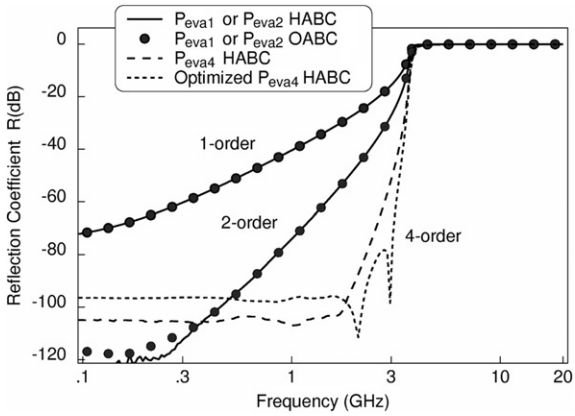

Fig. 9. Reflection from the end of the waveguide using operators (71) or (80), denoted as P_{eva1} and P_{eva2}, respectively, implemented either as an HABC or as an OABC. In the last two results, denoted as P_{eva4}, operator P_{eva2} is implemented with two HABCs.

reflections from the HABC and from the OABC are superimposed, as with Higdon operators in Fig. 6. But conversely to Fig. 6, here the evanescent waves are strongly absorbed while the traveling waves are totally reflected. Two additional results are reported in Fig. 9. The first one was computed using two HABCs, each one with operator (80). This was equivalent to a fourth-order operator ABC. The absorption is widely improved. The last result was also computed with two HABCs, but with different β's in place of unique value (79). One β was set to (79) and the other three were set using (77) and (78) in order that the reflection vanishes at frequencies 1, 2.5 and 3 GHz, respectively. As expected, at frequencies close to cut-off this optimized operator provides us with a better performance than with all the zero reflections set to zero frequency.

Considering results in Figs. 6 and 9, one can expect that combining operators (71) or (80) with Higdon operators, both traveling and evanescent waves will be absorbed. This can be easily realized by using several HABCs, or several HABCs and one OABC at the end of the domain. Results of calculations with such combinations are shown in Fig. 10. The first result is a combination of the first-order Higdon operator with (71). As expected the reflection is a combination of the first-order reflections observed in Figs. 6 and 9. The second result was obtained using (80) and the second-order Higdon operator. It is in accordance with results in Figs. 6 and 9, except at low frequency where the reflection grows. The origin of this low frequency spurious reflection that appears when combining operator (80) with Higdon operators is not understood. Finally, the third result was computed with three second-order HABCs and one second-order OABC, so that the global ABC was

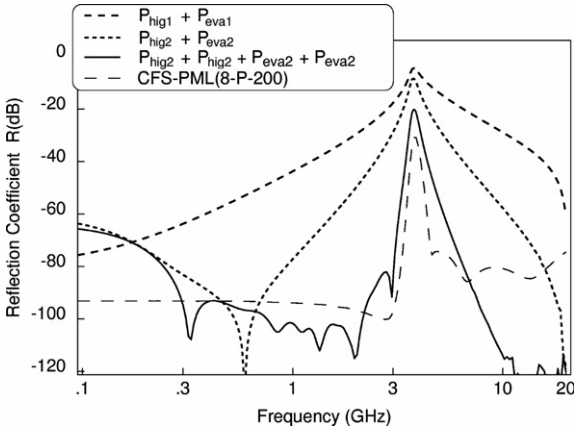

Fig. 10. Reflection from the end of the waveguide using various combinations of Higdon operators (P_{hig1} and P_{hig2}) with P_{eva1} and P_{eva2} operators (71) and (80). The third result was obtained using three HABCs and one OABC, as represented in Fig. 5.

equivalent to an eighth-order operator ABC. The second-order Higdon operator was used with the first two HABCs. Operator (80) was used with the third HABC and with the OABC (the β coefficients were those of the fourth-order optimized case in Fig. 9). The second HABC was implemented as a reversed Huygens surface (see Section 6.2 in the following for the definition of reversed surfaces). This reduces the above mentioned unexplained spurious low frequency reflection. As observed in Fig. 10, the attenuation is quite good at all the frequencies. The performance of this eighth-order ABC is close to that of the eighth-cell CFS-PML [8].

In summary, the Huygens ABC allows easy combinations of operators designed to absorb traveling waves with operators designed to absorb evanescent waves. This permits a quite good absorption of both kinds of waves in waveguide structures, like using the CFS-PML ABC. Notice that the operator designed for absorbing the evanescent waves depends on the mode to be absorbed (79), like the optimized α parameter of the CFS-PML [8]. From this the two ABCs may suffer from similar drawbacks if several modes have to be absorbed. Combinations of Higdon operators with operators (71) or (80) probably could be used for solving other problems where traveling waves and evanescent waves are separated with a transition or cut-off frequency, like in wave-structure interaction problems [7].

5.2. A combination of the Huygens ABC with the PML ABC

A unique feature of the HABC is the possibility of easy combinations with any other ABC, because the HABC can be placed in front of the other ABC. This has been done in the above where the HABC has been used in conjunction with an operator ABC. This can be also done with the PML ABC as illustrated in the following.

We consider the problem in Fig. 5. We now assume that the TM_0 mode is also present in addition to the TM_1 mode. The TM_0 mode has no cut-off, it is a traveling mode up to zero frequency. From this, if we use a CFS-PML optimized for the TM_1 mode [8], the TM_0 mode is not absorbed below the TM_1 mode cut-off. This is because the optimized CFS-PML is designed so as to be only a real stretch of coordinates below the cut-off, in order to reduce the numerical reflection of evanescent waves [8]. This is confirmed with results in Fig. 11 where only the TM_0 mode was exited in the guide. This mode is totally reflected at low frequency when using the CFS-PML optimized for the TM_1 mode. Conversely, using the Higdon operators with a HABC, the TM_0 mode is strongly absorbed.

The results in Fig. 12 were computed with both TM_0 and TM_1 modes in the waveguide (with the same magnitude). As expected, with the second-order Higdon HABC alone only the TM_0 mode is absorbed below TM_1 cut-off, resulting in a reflection of about -16 dB (natural decay of TM_1 and total absorbtion of TM_0). With the CFS-PML alone, the TM_1 mode is well absorbed at any frequency, but the TM_0 mode reflection is total at low frequency. With the first-order or second-order Higdon HABC placed in front of the CFS-PML, the two modes are very well absorbed, resulting in a quite small reflection over the whole frequency spectrum.

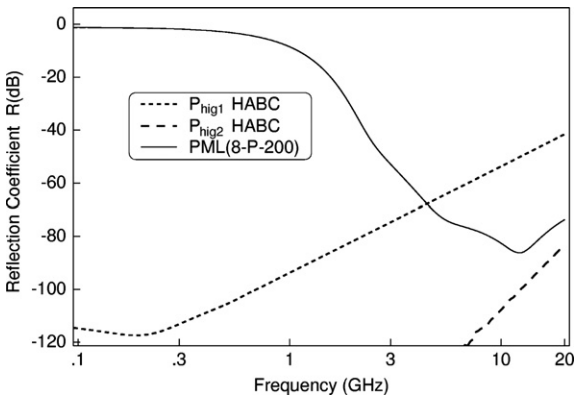

Fig. 11. Reflection of the TM_0 mode from the end of the waveguide, computed with the first-order or the second-order Higdon HABC, and with the PML ABC optimized for the TM_1 mode.

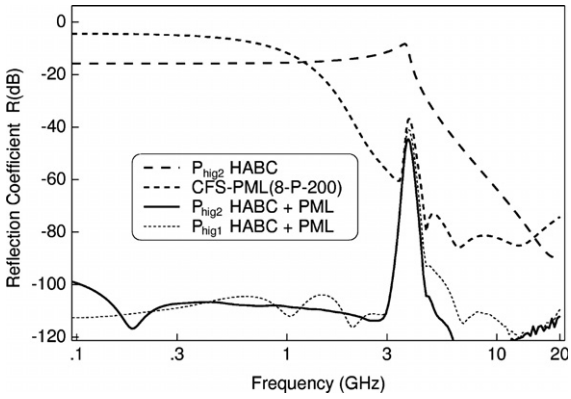

Fig. 12. Reflection from the end of the waveguide when TM_0 and TM_1 mode are present. Results are shown for waveguide terminations with a Higdon HABC, the CFS-PML and two combinations of the Higdon HABC with the CFS-PML.

In summary, the HABC can be easily used in conjunction with a PML ABC when facing specific challenging problems. The problem with TM_0 and TM_1 modes could be also addressed with only a CFS-PML by varying its α parameter, but using an HABC for absorbing the TM_0 mode is an alternative solution that is effective and simple. Notice that there exist other problems of electromagnetics where traveling and evanescent waves are present at the same frequency, as the scattering from periodic corrugated surfaces. They could be also addressed with a HABC-PML combination.

6. The re-radiating boundary condition (rRBC) and the multiple absorbing surfaces (MAS) ABC

In the following we briefly review ABCs [1–3] that are special cases of Huygens ABCs introduced in the present paper. We show that most numerical results reported in these papers can be interpreted using the theoretical properties of Huygens ABCs.

6.1. The re-radiating boundary condition (rRBC)

The rRBC relies on the introduction of the concept of teleportation of fields. The field one time step in the past and one space step backwards is "teleported" upon a Huygens surface to radiate a field opposite to the outgoing field. The teleported field is then identical to estimate (8) with δx and δt equal to the FDTD steps Δx and Δt. So, the rRBC is a Huygens ABC relying on the elementary operator (7) called space–time extrapolation in [5]. In addition, the computational domain is ended with an impedance condition called a Huygens termination in [2,3]. It can be easily shown that this condition is equivalent to a first-order operator ABC.

There is neither derivation nor theoretical prediction in [2,3], only FDTD experiments are provided. However, the authors observed that the pulse outside the rRBC resembles the derivative of the incident pulse. They used the terms derivation and re-integration to characterize the direct and reverse effects of the rRBC. Obviously, this is in accordance with theoretical predictions (14) and (21). Having in mind the fact that the rRBC relies on the elementary operator, most FDTD experiments in [2] can be easily interpreted. Consider for example Fig. 5 in [2]. With the rRBC and a PEC at the end of the domain, the reflection equals -9 dB. This is in a good accordance with the theoretical reflection from elementary operator (22) that yields -10 dB with $\Delta x = 2c\Delta t$ (the exact ratio $\Delta x/c\Delta t$ is not given in [2], it equals 2 in [3]). Adding the impedance termination the reflection drops to -37 dB because this condition is better than the elementary operator at normal incidence.

Reflection observed in Fig. 7 is also consistent with use of the elementary operator with the rRBC. From (31) the reflection from this operator vanishes at an incidence angle of 60° (assuming that $\Delta x = 2c\Delta t$). With three rRBCs, the reflection is the cube of (31). The relative insensitivity of the reflection in function of the incidence angle, as observed in Fig. 7 of [2], is probably due to this reflection coefficient whose best performance (zero reflection) is at wide incidence, around 60°.

Numerous experiments reported in [3] show that the rRBC performance can be close to that of the PML ABC. However, generalization of the conclusions of these tests is questionable, because they were performed in a 2D domain with the electric field perpendicular to the domain. It is known that any ABC performs very well with this kind of problems, because no evanescent waves have to be absorbed. For example, Higdon and Engquist–Majda [10] ABCs also yield quite good absorption in that case [11]. In realistic FDTD applications where evanescent waves are present, results with the rRBC would be far poorer, because the elementary operator reflects in totality evanescent waves, as shown theoretically (53) and confirmed with waveguide experiments like the ones in Fig. 6.

6.2. The multiple absorbing surface (MAS)

The absorbing surface concept in [1] is introduced in the FDTD method without explicit reference to equivalent currents radiating a field opposite to the outgoing field. Nevertheless, in continuous spaces it is equivalent to the Huygens ABC in Figs. 1 or 2. The estimate of the incident field at Huygens surface location is computed using the first-order Higdon operator.

The field transmitted through the Huygens surface is derived in [1]. Although the field components are set at nodes of the FDTD grid, the derivation is performed in the continuous space, with harmonic waves, like in Section 3.2 of the present paper. The author was close to discovering that the transmitted wave is the derivative of the incident wave. Indeed, by expanding the exponentials in formula (23) of [1] the transmission coefficient becomes proportional to $j\omega$, like in (30). More precisely, formula (B.2) in Appendix B is obtained with $j\omega$ in place of the derivative (and with $w = -p$ due to different notations). Similarly, expanding the exponentials in (26) of [1], formula (B.3) is obtained with $1/j\omega$ in place of the integral. However, strictly speaking the derivations in [1] are not correct, because they assume that the incident field is known at Huygens surface location. This is not possible as discussed in Section 3.5 in the above and in Appendix B, so that the exact field is replaced with the estimated field. From this and from derivations in Appendix B, coefficients $1/(1-p)$ and $1-p$ are missing in transmissions (23) and (26) in [1]. Nevertheless, the overall reflection in [1] is correct, because it equals the product of the two transmissions. From this, an important conclusion in [1] is correct, that is the reflection from the Higdon MAS ABC is identical, rigorously, to the reflection from the corresponding Higdon operator used as an ABC.

Several absorbing surfaces are stacked in [1], so as to increase the absorption, and the concept of pairs of Huygens surfaces is introduced. The first surface of a pair is the regular surface, like in Figs. 1 and 2. The second one is reversed. It is implemented as if the field to be absorbed were an ingoing field. From the point of view of the overall reflection of the outgoing field, such a reversed Huygens surface is equivalent to the regular one. Its overall reflection coefficient is the same. The difference is only that the outgoing field is first integrated, and second derived as it passes back through the surface. It is claimed in [1] that such pairs of surfaces remove the instability observed by the author as using several surfaces. In our computations we never observed instability, even as using four second-order surfaces in the case in Fig. 10. However, our experiments were only 2D experiments with waveguide problem in Fig. 5 where there is no corner region. May be the instability arises from the corner regions. Nevertheless, we tested a pair of surfaces like in [1] and we observed a significant reduction of the low frequency spurious reflection observed when Higdon operators are used in conjunction with operators (71) or (80), like in the eighth-order case in Fig. 10.

As in [2,3], the experiments with a source point in a 2D domain reported in Fig. 9 of [1] yield attenuations as good as using a PML ABC. But once again such experiments do not correspond to most situations of computational electromagnetics, because of lack of evanescent waves. Even by stacking a large number of absorbing surfaces, as long as only Higdon operators are used to estimate the outgoing field, the performance of the MAS method would be poor if the MAS surfaces were placed in the evanescent region. As we have shown in the above, use of an operator designed for the absorbtion of evanescent waves is needed in such situations. The last experiment in Fig. 10 of [1] also shows a very good agreement with the PML ABC, with both ABCs placed quite close to a scattering sphere. Such a good agreement is due to the fact that the frequency of interest is close to the resonance of the sphere, so that the field surrounding the sphere is weakly evanescent. At lower frequency the field becomes strongly evanescent and the performance of the MAS method probably would severely deteriorate.

7. Conclusion

In this paper we have investigated absorbing boundary conditions called Huygens ABCs that hold as special cases the previously published MAS [1] and rRBC [2,3]. The theoretical features of the Huygens ABCs have been derived. The most important feature is that the Huygens ABCs are equivalent, in theory, to previously known operator ABCs. From this, Huygens ABCs are not novel ABCs, they are rather new implementations of previously used operator ABCs.

However, the interest of Huygens ABCs seems larger than that of operator ABCs, because a HABC can be easily combined with other HABCs or with any other ABC. As reported in [1,2], HABCs equivalent to high-order operator ABCs can be realized with no stability problem for the absorption of traveling waves up to wide angles of incidence. In this paper we have shown that HABCs also allow operators designed to absorb evanescent waves to be combined with regular operators designed to absorb traveling waves. This permits problems where both evanescent and traveling waves are present to be addressed in a satisfactory manner, like with a PML ABC. Especially, an experiment has been provided with a HABC equivalent to an eighth-order operator ABC, with four orders devoted to the absorption of evanescent waves and four orders devoted to the absorption of traveling waves. Another possible application of HABCs lies in the easy combination of an HABC with a PML ABC. As shown by an experiment, this can be very well suited to address some special problems where both evanescent and traveling waves are present at the same frequencies.

In conclusion, the Huygens ABC concept is a promising implementation of operator ABCs. In waveguide problems, by using operators designed to absorb evanescent waves the performance of the Huygens ABC can be close to that of the PML ABC, in terms of the effectiveness of the absorption and in terms of the needed computational resource. However, further works are needed so as to compare in a more exhaustive manner the Huygens ABC with the PML ABC. What we can say now is that the Huygens ABC is probably an ABC that can challenge the PML ABC, at least in some classes of applications.

Appendix A. Operators without first-order term

Let us consider the following operator:

$$P = K(-\delta x) + K(-\delta x)Z(-\delta t) - K(-2\delta x)Z(-\delta t) \tag{A.1}$$

that is of the form (4). For a wave propagating to the right, the corresponding estimate (2) reads

$$\widetilde{U}(x_c,t) = U_{i+}(x_c-\delta x,t) + U_{i+}(x_c-\delta x,t-\delta t) - U_{i+}(x_c-2\delta x,t-\delta t) \tag{A.2}$$

In place of first-order expansions like (11), we use here second-order expansions of the three terms to the right-hand side of (A.2). This yields

$$\begin{aligned}\widetilde{U}(x_c,t) = {} & U_{i+}(x_c,t) - \frac{\partial U_{i+}(x_c,t)}{\partial x}\delta x + \frac{1}{2}\frac{\partial^2 U_{i+}(x_c,t)}{\partial x^2}\delta x^2 + \left[U_{i+}(x_c,t) - \frac{\partial U_{i+}(x_c,t)}{\partial x}\delta x - \frac{\partial U_{i+}(x_c,t)}{\partial t}\delta t\right.\\ & \left. + \frac{1}{2}\frac{\partial^2 U_{i+}(x_c,t)}{\partial x^2}\delta x^2 + \frac{1}{2}\frac{\partial^2 U_{i+}(x_c,t)}{\partial t^2}\delta t^2 + \frac{\partial^2 U_{i+}(x_c,t)}{\partial t\partial x}\delta x\delta t\right]\\ & - \left[U_{i+}(x_c,t) - \frac{\partial U_{i+}(x_c,t)}{\partial x}2\delta x - \frac{\partial U_{i+}(x_c,t)}{\partial t}\delta t + \frac{1}{2}\frac{\partial^2 U_{i+}(x_c,t)}{\partial x^2}4\delta x^2 + \frac{1}{2}\frac{\partial^2 U_{i+}(x_c,t)}{\partial t^2}\delta t^2\right.\\ & \left. + \frac{\partial^2 U_{i+}(x_c,t)}{\partial t\partial x}2\delta x\delta t\right]\end{aligned}$$

The sum of the first-order terms is zero so that the expansion reduces to

$$\widetilde{U}(x_c,t) = U_{i+}(x_c,t) - \frac{\partial^2 U_{i+}(x_c,t)}{\partial x^2}\delta x^2 - \frac{\partial^2 U_{i+}(x_c,t)}{\partial x\partial t}\delta x\delta t \tag{A.3}$$

Using (A.3) into (9) yields

$$U_{t+}(x_{c+},t)=\frac{\partial^2 U_{i+}(x_c,t)}{\partial x^2}\delta x^2+\frac{\partial^2 U_{i+}(x_c,t)}{\partial x\partial t}\delta x\delta t \tag{A.4}$$

Replacing then the derivatives on space with derivatives on time, we obtain

$$U_{t+}(x_{c+},t)=-\frac{\partial^2 U_{i+}(x_c,t)}{\partial t^2}\frac{\delta x}{c}\left(\delta t-\frac{\delta x}{c}\right) \tag{A.5}$$

From this, the field transmitted through the Huygens surface is proportional to the second derivative of the incident field, in place of the first derivative with the elementary operator or in the general case (2)–(4). This has been verified with a FDTD experiment like the one in Fig. 4. Then, with (A.1) in place of (7) for estimating the field on the Huygens surface, the wave outside the Huygens surface, at point B, was in a perfect agreement with (A.5), i.e. it was the second derivative of the Gaussian pulse multiplied with coefficient in (A.5).

Let us now consider the wave propagating to the left, as in Fig. 2b. An expansion to the second-order like in the above yields

$$\widetilde{U}(x_c,t)=U_{t-}(x_{c-},t)-\frac{\partial^2 U_{t-}(x_{c-},t)}{\partial x^2}\delta x^2-\frac{\partial^2 U_{t-}(x_{c-},t)}{\partial x\partial t}\delta x\delta t \tag{A.6}$$

Inserting this into (15) we have

$$\frac{\partial^2 U_{t-}(x_{c-},t)}{\partial x^2}\delta x^2+\frac{\partial^2 U_{t-}(x_{c-},t)}{\partial x\partial t}\delta x\delta t=U_{i-}(x_c,t_c) \tag{A.7}$$

that yields, after replacement of the derivatives on space with derivatives on time

$$U_{t-}(x_{c-},t)=\frac{1}{\frac{\delta x}{c}\left(\delta t+\frac{\delta x}{c}\right)}\int\int U_{i-}(x_c,t')\,\mathrm{d}t'^2 \tag{A.8}$$

Finally, in the case of Fig. 2c, where an incident wave propagating to the right is reflected from $U=0$ condition, using (A.5) and (A.8), the overall reflection is

$$r=-\frac{\Delta x-c\Delta t}{\Delta x+c\Delta t} \tag{A.9}$$

This is the reflection from operator (A.1) used as an operator ABC. This could be easily derived in a direct manner. This is also trivial because operator (A.1) is the complementary operator [12,13] of the elementary operator (7), so that their reflections are opposite, as observed by comparing (A.9) with (22).

In the case of general operator (4), by expanding the field to the second-order like in the above, and by assuming that the first-order terms equal zero, the following transmitted field is obtained:

$$U_{t+}(x_{c+},t)=-\frac{\partial^2 U_{i+}(x_c,t)}{\partial t^2}\sum_{k=1}^{N}a_k\left(\frac{\cos^2\theta\delta x_k^2}{2c^2}+\frac{\delta t_k^2}{2}-\frac{\cos\theta\delta x_k\delta t_k}{c}\right) \tag{A.10}$$

in place of (34). Similarly, for the wave propagating to the left, we obtain

$$U_{t-}(x_{c-},t)=-\frac{1}{\sum_{k=1}^{N}a_k\left(\frac{\cos^2\theta\delta x_k^2}{2c^2}+\frac{\delta t_k^2}{2}+\frac{\cos\theta\delta x_k\delta t_k}{c}\right)}\int\int U_{i-}(x_c,t')\,\mathrm{d}t'^2 \tag{A.11}$$

so that the overall reflection from the HABC reads

$$r=-\frac{\sum_{k=1}^{N}a_k\left(\cos^2\theta\delta x_k^2+c^2\delta t_k^2-2\cos\theta\delta x_k c\delta t_k\right)}{\sum_{k=1}^{N}a_k\left(\cos^2\theta\delta x_k^2+c^2\delta t_k^2+2\cos\theta\delta x_k c\delta t_k\right)} \tag{A.12}$$

in place of (37) that equals zero in the absence of first-order term in the expansion of the field. It can be shown that (A.12) is also the reflection from the same operator used as an operator ABC. Notice that (A.9) is consistent with (A.12) for $\theta=0$, i.e. using a_k coefficients and shifts in (A.1) into (A.12) yields (A.9).

In summary, there exist operators of the form (4) with which the first-order term is absent in the expansion of the field. This arises when the number of shifts with positive sign equals the number of shifts with negative

sign, for both space and time. This is the case with (A.1) where there are two positive and two negative space shifts, and one positive and one negative time shifts. The absence of the first-order term has no significant impact on the major conclusion, which is the fact that the overall reflection from the HABC is identical to the reflection from the corresponding operator ABC.

Appendix B. Higdon operators and extension of the general operator

Let us consider the incident wave propagating to the right in Fig. 2a. Using operator (40a) in place of (7) and expansions like (11), if the incident field were known at Huygens surface location, estimate (6) would be

$$\widetilde{U}(x_c,t) = U_{i+}(x_c,t) - \frac{\partial U_{i+}(x_c,t)}{\partial x}\delta x - \frac{\partial U_{i+}(x_c,t)}{\partial t}\delta t + wU_{i+}(x_c,t) - w\frac{\partial U_{i+}(x_c,t)}{\partial x}\delta x - wU_{i+}(x_c,t) + w\frac{\partial U_{i+}(x_c,t)}{\partial t}\delta t \tag{B.1}$$

Inserting (B.1) into (9) yields the transmitted field

$$U_{t+}(x_{c+},t) = \left[(1-w)\delta t - (1+w)\frac{\delta x}{c}\right]\frac{\partial U_{i+}(x_c,t)}{\partial t} \tag{B.2}$$

It can be easily verified that (B.2) is consistent with (34) for $\theta = 0$, i.e. using a_k coefficients in (40a) into (34) yields (B.2).

For a wave propagating to the left, a similar derivation yields

$$U_{t-}(x_{c-},t) = \frac{1}{(1-w)\delta t + (1+w)\frac{\delta x}{c}}\int U_{i-}(x_c,t')\,\mathrm{d}t' \tag{B.3}$$

The overall reflection from the Huygens ABC is then

$$r = -\frac{(1-w)c\delta t - (1+w)\delta x}{(1-w)c\delta t + (1+w)\delta x} \tag{B.4}$$

It can be verified with a_k coefficients in (40a) that (B.3) and (B.4) are special cases of (36) and (37). Using (40b) and replacing δx with $\cos\theta\delta x$ so as to extend the above 1D derivation to the 2D or 3D cases, (B.4) gives the well known reflection from a Higdon operator ABC [6]

$$r = \frac{\cos\theta_1 - \cos\theta}{\cos\theta_1 + \cos\theta} \tag{B.5}$$

where θ_1 is the incidence where the reflection is zero.

Unfortunately, in the actual use of the Higdon operator, estimate (B.1) cannot be implemented, because the exact incident field $U_{i+}(x_c, t-\delta t)$ is not known due to the discontinuity of the total field at x_c. From this, $U_{i+}(x_c, t-\delta t)$ is replaced with its estimate $\widetilde{U}(x_c, t-\delta t)$, that is the estimate at previous time step with a finite-difference method. From this, the following replaces (B.1):

$$\widetilde{U}(x_c,t) = U_{i+}(x_c,t) - \frac{\partial U_{i+}(x_c,t)}{\partial x}\delta x - \frac{\partial U_{i+}(x_c,t)}{\partial t}\delta t + wU_{i+}(x_c,t) - w\frac{\partial U_{i+}(x_c,t)}{\partial x}\delta x - w\widetilde{U}(x_c,t) + w\frac{\partial \widetilde{U}(x_c,t)}{\partial t}\delta t \tag{B.6}$$

Since $\widetilde{U}$ is a first-order estimate of U_{i+}, we can write

$$\frac{\partial \widetilde{U}(x_c,t)}{\partial t}\delta t = \frac{\partial U_{i+}(x_c,t)}{\partial t}\delta t + 0(\delta x\delta t) + 0(\delta t^2) \tag{B.7}$$

so that $\widetilde{U}$ can be replaced with U_{i+} in the derivative of the last term in (B.6), with only a second-order error. This yields

$$(1+w)\widetilde{U}(x_c,t) = (1+w)U_{i+}(x_c,t) - (1+w)\frac{\partial U_{i+}(x_c,t)}{\partial x}\delta x - (1-w)\frac{\partial U_{i+}(x_c,t)}{\partial t}\delta t \tag{B.8}$$

Inserting this into (9), the following transmitted field is obtained:

$$U_{t+}(x_{c+},t)=\frac{1}{1+w}\left[(1-w)\delta t-(1+w)\frac{\delta x}{c}\right]\frac{\partial U_{i+}(x_c,t)}{\partial t} \tag{B.9}$$

that differs from (B.2) with coefficient $1/(1+w)$. For the wave propagating to the left, a similar derivation yields

$$U_{t-}(x_{c-},t)=\frac{1+w}{(1-w)\delta t+(1+w)\frac{\delta x}{c}}\int U_{i+}(x_c,t')\,\mathrm{d}t' \tag{B.10}$$

that differs from (B.3) with coefficient $(1+w)$. From (B.9) and (B.10), the overall reflection from the Higdon HABC remains given by (B.4) or (B.5). In summary, since (B.2), (B.3), (B.4) are special cases of (34), (36), (37), respectively, due to the replacement of the exact field with its estimate the field outside the HABC is divided with $(1+w)$ in comparison with value predicted with (34), it is multiplied with $(1+w)$ in comparison with (36) as it passes back through the Huygens surface, and at the end the overall reflection is still predicted by the reflection of operator (4), that is (37).

The above derivations can be reproduced with any operator (4). Assuming that $\delta x_k=0$ for its first M terms, operator (4) can be rewritten as

$$P=\sum_{k=1}^{M}a_kZ(-\delta t_k)+\sum_{k=M+1}^{N}a_kK(-\delta x_k)Z(-\delta x_k) \tag{B.11}$$

This leads to the following transmitted field for the wave propagating to the right:

$$U_{t+}(x_{c+},t)=\frac{\partial U_{i+}(x_c,t)}{\partial t}\frac{1}{Q}\sum_{k=1}^{N}a_k(\delta t_k-\cos\theta\delta x_k/c) \tag{B.12}$$

where

$$Q=1-\sum_{k=1}^{M}a_k \tag{B.13}$$

In comparison with (34), the transmitted field is divided with coefficient Q. Notice that (B.9) is consistent with (B.12), i.e. using $M=1$ and $a_1=-w$ in (B.12), (B.13), for $\theta=0$ we obtain (B.9). For the wave propagating to the left, the derivation yields (36) multiplied with coefficient (B.13). And at the end, the overall reflection from the HABC remains given by (37), with obviously $\delta x_k=0$ for $k\leqslant M$.

In conclusion to the above, we can extend the definition of operator (4) to $\delta x_k\leqslant 0$, with the exact field replaced with its estimate in (2) if $\delta x_k=0$. The overall reflection (37) is always valid. As a corollary, we can consider that Higdon operators are special cases of general operator (4).

Two 1D experiments like in Fig. 4 were performed with the Higdon operator in place of the elementary operator. With $w=-0.268$ and $w=+0.318$, corresponding to 3D zero reflection at incidences 30° and 75°, respectively, the transmitted wave was in a perfect agreement with (B.9), i.e. the presence of coefficient $1/(1+w)$ was very well verified. And the magnitude of the wave reflected back to the inner domain was in agreement with (B.4).

References

[1] I. Wayan Sudiarta, An absorbing boundary condition for FDTD truncation using multiple absorbing surfaces, IEEE Trans. Antennas Propag. 51 (2003) 3268–3275.
[2] R.E. Diaz, I. Scherbatko, A simple stackable re-radiating boundary condition (rRBC) for FDTD, IEEE Antennas Propag. Magazine 46 (1) (2004) 124–130.
[3] R.E. Diaz, I. Scherbatko, A new multistack radiation boundary condition for FDTD based on self-teleportation of fields, J. Comput. Phys. 203 (2005) 176–190.
[4] A. Taflove, S. Hagness, Computational Electrodynamics: The Finite-difference Time-domain Method, Artech House, Boston, 2000.
[5] R. Higdon, Absorbing boundary conditions for difference approximations to the multi-dimensional wave equation, Math. Comput. 47 (1986) 437–459.

[6] R. Higdon, Numerical absorbing boundary conditions for the wave equation, Math. Comput. 49 (1987) 65–90.
[7] J.-P. Bérenger, Numerical reflection from FDTD-PML's: a comparison of the split PML with the unsplit and CFS PML's, IEEE Trans. Antennas Propag. 50 (2002) 258–265.
[8] J.-P. Bérenger, Application of the CFS PML to the absorption of evanescent waves in waveguides, IEEE Micr. Wireless Compon. Lett. 6 (2002) 218–220.
[9] J.-P. Bérenger, A Huygens subgridding for the FDTD method, IEEE Trans. Antennas Propag. 54 (2006) 3797–3804.
[10] B. Engquist, A. Majda, Radiation boundary condition for the numerical simulation of waves, Math. Comput. 31 (1977) 629–651.
[11] J. Blaschak, G. Kriegsmann, A comparative study of absorbing boundary conditions, J. Comput. Phys. 77 (1988) 109–139.
[12] O.M. Ramahi, Complementary operators: a method to annihilate artificial reflections arising from the truncation of the computational domain in the solution of partial differential equations, IEEE Trans. Antennas Propag. 43 (1995) 697–704.
[13] O.M. Ramahi, Complementary boundary operator for wave propagation problems, J. Comput. Phys. 133 (1997) 113–128.